Temperature and Concentration Effects on Li+− Ion Hydration. A Molecular Dynamics Simulation Study

ARTICLE *in* THE JOURNAL OF PHYSICAL CHEMISTRY B · MARCH 2003

Impact Factor: 3.3 · DOI: 10.1021/jp026677l

6 AUTHORS, INCLUDING:

Andrei Komolkin
Saint Petersburg State University
23 PUBLICATIONS **436** CITATIONS
SEE PROFILE

Pavel V Yushmanov
KTH Royal Institute of Technology
11 PUBLICATIONS **152** CITATIONS
SEE PROFILE

Alexander P Lyubartsev
Stockholm University
155 PUBLICATIONS **4,706** CITATIONS
SEE PROFILE

Temperature and Concentration Effects on Li^+-Ion Hydration. A Molecular Dynamics Simulation Study

A. V. Egorov,[†] A. V. Komolkin,[†] V. I. Chizhik,[†] P. V. Yushmanov,[†] A. P. Lyubartsev,[‡] and Aatto Laaksonen*,[‡]

Institute of Physics, St. Petersburg University, 198504, St. Petersburg, Russia, and Division of Physical Chemistry, Arrhenius Laboratory, Stockholm University, Stockholm S 106 91, Sweden

Received: August 3, 2002; In Final Form: January 31, 2003

Molecular dynamics simulations of aqueous LiCl solution have been carried out over wide concentration (from 0.1 to 11.4 mol/kg) and temperature (from −30 to 110 °C) ranges. Three different interaction potentials are investigated: the recent Li^+−water effective pair potential, derived from ab initio molecular dynamics simulations [Lyubartsev, A. P.; Laasonen, K.; Laaksonen, A. *J. Chem. Phys.* **2001**, *114*, 3120], as well as earlier potentials of Lennard-Jones type with two widely different sets of parameters [Dang, L. X.; *J. Chem. Phys.* **1992**, *96*, 6970 and Heinzinger, K.; *Physica B* **1985**, *131*, 196]. Hydration structure and residence times around Li^+ are studied with focus on the still somewhat controversial issue of hydration structure: both tetrahedral and octahedral water coordination have been predicted from the experiments. Besides classical MD simulations, even complementary Car−Parrinello simulations were employed to investigate the stability of a possible six-coordinated hydration shell around lithium. Self-diffusion coefficients for lithium were calculated for Li^+ from the simulations and compared to NMR spin−echo measurements. The new ab initio-based exponential Li^+−H_2O interaction potential appears to be robust giving the overall characteristic hydration properties in agreement with experiments. However, while it reproduces the radial distribution function (RDF) features from a recent neutron diffraction with isotopic substitution (NDIS) experiments with a well-pronounced tetrahedral water structure, the same experiment is interpreted to give octahedral water structure around lithium at the same concentrations and temperatures as were used in our simulations.

1. Introduction

Understanding the microstructure of aqueous electrolyte solutions and understanding hydration phenomenon of the ions in particular are problems of fundamental interest in chemistry and chemical engineering. Because of many difficulties in experimental studies and their interpretations, the existing experimental data of microscopic characteristics obtained from these highly nonideal solutions are often incomplete or contradictive. This is true even for the most basic characteristics of ion hydration, namely, the hydration number. In the case of lithium ion, X-ray and neutron scattering experiments (see refs 1−3 and references therein) have suggested both tetrahedral and octahedral coordination of Li^+ ion in water. Interpretation of Raman measurements[4] indicates a hydration number equal to four. Variable concentration and temperature ^1H and ^7Li NMR relaxation studies of aqueous LiCl solutions suggest[5] that the structure of the first coordination shell around the lithium ion undergoes a reorganization between 30 and 40 °C, the coordination number changing from 4 to 6 as the temperature is raised.

Molecular dynamics (MD) computer simulations are capable of providing detailed information of all atoms in the simulated system, now typically on a few nanoseconds time scale, which is enough to compute the averages of microscopic characteristics of interest. Of course, it should be kept in mind that computer simulations are always as good as the used potential models describing the interactions between the molecules. In the case of aqueous ionic solutions, there exist a fairly impressive amount of different interaction models, yielding often widely spread results for the calculated properties. This is reflected in an extensive number of computer simulation studies of Li^+ solutions (both classical MD and Monte Carlo),[6−45] all of them reporting a broad variety of results obtained with different ion−water potental models and furnished with very different parameters. A major part of the Li^+−water potentials suggested in the literature are of standard Lennard-Jones type,[6,7,19,22,38,46−50] while there are also potentials including terms with other powers of $1/r$,[12,40] as well as more complicated potentials with exponential short-range repulsion,[18,20,21,36,41,51] all leading to different results and conclusions. For example, the lithium coordination number varies from 4[20,26−28,30,34,35,38,40,42] to 6.[10,13,18,21,31,36,37,41,43]

Quantum chemical calculations[51−54] predict that Li^+ has four inner shell water neighbors. Also, ab initio molecular dynamics simulations of lithium ion in water[41,55−57] suggest a 4-fold lithium hydration. In ab initio MD simulations, the forces are determined directly from quantum chemical calculations without any interaction potentials. It is therefore tempting to believe that these types of simulations are more reliable than classical molecular dynamics simulations. However, quantum chemical or ab initio calculations are computationally very expensive and provide therefore only a limited statistical sampling. Typically, only a few tens of picoseconds can be covered currently by Car−Parrinello MD simulations. It is not really enough to provide any reliable results, for example, for transport properties such as the self-diffusion coefficients.

* To whom correspondence should be addressed. E-mail: aatto@physc.su.se.
[†] St. Petersburg University.
[‡] Stockholm University.

10.1021/jp026677l CCC: $25.00
Published on Web 03/19/2003

The main goal of the present study is to perform a systematic investigation of temperature and concentration effects on Li^+-ion hydration using classical MD simulations. We have carried out simulations of aqueous LiCl solutions over a wide range of temperatures (from −30 to 110 °C) and concentrations (from 0.1 to 11.4 mol/kg) using three different ion−water potentials and compared the results with experiments to test the validity of the models. One of the potential models is new[57] and obtained from Car−Parrinello MD simulations by using the method of inverse Monte Carlo.[58]

The paper is organized as follows. In section 2, we describe the computational aspects, simulation models, and experimental details. Results and discussion are given in sections 3 and 4, while conclusions are summarized in section 5.

2. Methods

2.1. Ion−Water Interaction Potential. In computer simulations, the choice of interaction potentials is critical for the correct description of the investigated system. Usually the potential functions are parametrized by fitting the energies from quantum chemical calculations or experiments, if available. Recently, a novel approach was suggested to derive classical interaction potentials from ab initio simulation data.[59] The main idea behind this approach is to apply first the inverse Monte Carlo procedure to reconstruct the interaction potential from radial distribution functions generated in ab initio simulations.[58] In a recent paper,[57] an effective Li^+−water interaction potential was constructed on the basis of Car−Parrinello MD simulations. When this potential is used in classical MD or MC simulations, it reproduces the very same lithium−water oxygen radial distribution functions as were obtained in the parent ab initio simulation.

The nonelectrostatic short-range part of the Li^+−water oxygen potential has been fitted to a simple, single-exponential form:

$$V_{\text{eff}}(r) = A \exp(-Br) \tag{1}$$

with $A = 37\,380$ kJ/mol and $B = 3.63$ Å^{-1}. For simplicity, we call this exponential ab initio potential here below for "EAI" in lack of any better notation.

For a comparison we have also chosen two other, commonly used standard Lennard-Jones type of Li^+−water potentials, one parametrized by Dang[30] (giving coordination number 4) and another reported by Heinzinger[48] (giving six-coordinated water shell).

2.2. Computational Details. The simulations of aqueous LiCl solutions were carried out in a canonical *NVT* ensemble in a cubic periodic cell. Temperature was kept constant by using the Nosé−Hoover method.[60,61] The equations of motion were solved using the standard Verlet leapfrog algorithm with a time step of 1.0 fs. The long-range Coulomb forces are calculated using the Ewald summation method. The simulations were performed at eight different salt concentrations. Each configuration was preliminary equilibrated during a 200 ps run. The characteristic simulation parameters are given in Table 1. System 4 (concentration 1.72 mol/kg) was studied at temperatures ranging from −30 to 110 °C, and each temperature point was simulated for 2.0 ns.

As the water model, we have used the SPC/E water model[63] in which the hydrogens have no Lennard-Jones parameters, thus interacting with other atoms (carrying a charge) only through the electrostatic forces. The SPC/E water model has been shown to describe the temperature dependence of self-diffusion in pure water[64,65] reasonably well. To describe the nonelectrostatic part of the Cl^-−water and the ion−ion interactions the Lennard-Jones potential is used. The corresponding parameters are taken from ref 48 for our EAI model and Heinzinger's lithium−water potentials and from ref 66 for the Dang potential. Standard Lorentz−Berthelot combination rules were used to describe the cross-interactions. All potential models, except our EAI model, are of "12-6-1" type in which a Lennard-Jones potential is used to describe the short-range interactions and a Coulomb term is used for the long-range electrostatic interactions.

TABLE 1: Characteristic Simulation Parameters

	system							
	1	2	3	4	5	6	7	8
no. of H_2O molecules	341	337	331	323	303	283	263	243
no. of ion pairs	1	3	6	10	20	30	40	50
salt concn, mol/kg	0.16	0.50	1.01	1.72	3.67	5.89	8.45	11.43
density[a], g/cm^3	1.003	1.010	1.022	1.039	1.076	1.115	1.156	1.196
simulation time, ns	3.0	3.0	2.0	2.0	2.0	2.0	2.0	2.0

[a] Densities were taken from ref 62.

The coordination number of lithium ion is calculated as the integral of the ion−water oxygen radial distribution function from 0 to its first minimum. The self-diffusion coefficients are obtained from the mean square displacements of the molecules. The residence times of water molecules in lithium ion hydration shell are calculated following the standard procedure described in refs 15 and 67. We do not consider the hydration of the chloride ions in this work because we concentrate on the more intriguing lithium cation.

2.3. Experimental Methods. Because the experimental data on temperature effect on lithium diffusion in low-concentration aqueous LiCl solutions are very incomplete (see, for instance, ref 68 and references therein), we have measured the temperature dependence of lithium self-diffusion coefficient in 1.7 mol/kg LiCl aqueous solution. The self-diffusion coefficients were obtained by means of ^{7}Li NMR spin−echo experimental techniques. The solution was prepared by dilution of the saturated LiCl aqueous solution at room temperature in doubly distilled water. The measurements were performed by a standard static field gradient spin−echo method (for its detailed description, see ref 69) using a Bruker SXP 4-100 pulse spectrometer operating at 35 MHz (^{7}Li) and 90 MHz (^{1}H). If one applies the steady magnetic field gradient, the NMR spin−echo amplitude at time τ is given by

$$A(t) = A(0) \exp(-t/T_2) \exp(-\gamma^2 G^2 D t^3/12)$$

where G is the magnetic field gradient, T_2 is the transversal relaxation time of the investigated nucleus, γ is its gyromagnetic ratio, and D is the self-diffusion coefficient. The gradient was produced by the Helmholtz coils. The current was generated by conventional power supply ($\Delta I/I \leq 10^{-3}$). In our experiments, we have varied the value of the magnetic field gradient, which was calibrated against the self-diffusion coefficient of pure water, which is known with high accuracy.[70] The error limits for the sample temperature were within 0.5 K. The precision of the results varied but was not worse than 10%. The obtained experimental results for the lithium ion self-diffusion at different temperatures are given in Table 2.

TABLE 2: Lithium Self-Diffusion Coefficients in 1.7 *m* Aqueous LiCl Solution Obtained Using the NMR Spin−Echo Technique

t, °C	*T*, K	D_{Li}, 10^5 cm^2/s
−8.5	265	0.26
−2	271	0.43
9	282	0.68
22	295	0.87
33	306	1.33
49.5	333	2.03
71	344	2.88
83.5	357	3.74

TABLE 3: Some Properties of Aqueous LiCl Solution calculated at Different Concentrations[a]

Li^+-H_2O potential	concentration, mol/kg							
	0.16	0.50	1.01	1.72	3.67	5.89	8.45	11.43
	E_{tot}/N_{tot}, kJ/mol							
D	−49.2	−53.9	−60.9	−70.2	−93.6	−116.8	−139.6	−162.0
H	−48.8	−52.8	−58.8	−66.8	−86.8	−106.7	−126.4	−145.7
E	−48.9	−53.1	−59.3	−67.6	−88.2	−108.8	−129.0	−149.0
	$E(H_2O-H_2O)/N_{H_2O}$, kJ/mol							
D	−48.1	−44.0	−40.4	−34.2	−21.6	−20.1	−8.2	−1.2
H	−47.9	−44.6	−39.3	−34.5	−21.6	−9.4	−1.6	0.3
E	−48.3	−44.6	−39.4	−34.7	−21.3	−7.0	3.9	8.9
	$E(Li-H_2O)/N_{Li}$, kJ/mol							
D	−821	−778	−603	−557	−530	−422	−364	−266
H	−732	−642	−574	−508	−444	−409	−337	−256
E	−734	−671	−617	−533	−478	−481	−439	−364
	$E(Li-Cl)/N_{Li}$, kJ/mol							
D	−74	−273	−580	−972	−1829	−2860	−3864	−5067
H	−75	−288	−537	−900	−1766	−2699	−3772	−4899
E	−91	−261	−553	−914	−1767	−2667	−3683	−4755
	Coordination Number of Li^+							
D	4.12	4.13	3.94	3.90	3.88	3.55	3.25	2.82
H	5.55	5.53	5.47	5.40	5.29	5.08	4.56	4.02
E	4.03	4.04	4.02	3.98	3.99	3.92	3.77	3.53
	H_2O Self-Diffusion Coefficients (10^{-5} cm^2/s)							
D	2.11	2.04	1.89	1.70	1.18	0.82	0.48	0.32
H	2.15	2.10	1.93	1.69	1.23	0.83	0.46	0.23
E	2.21	2.04	1.93	1.73	1.26	0.86	0.49	0.24
	Li^+ Self-Diffusion Coefficients (10^{-5} cm^2/s)							
D	1.09	0.77	0.74	0.74	0.42	0.33	0.15	0.07
H	1.19	0.75	0.84	0.68	0.50	0.31	0.17	0.09
E	0.94	0.80	0.81	0.63	0.56	0.38	0.21	0.10
	H_2O-Li^+ Residence Times (ps)							
D	29.0	30.4	32.7	30.3	34.3	37.3	38.9	41.0
H	17.3	18.2	17.9	18.1	20.1	21.6	23.5	26.2
E	26.8	26.8	26.2	25.5	23.9	22.9	23.6	24.3

[a] Notation: D = Dang parameters;[30] H = Heinzinger parameters;[48] E = our own exponential ab initio-based Li^+-H_2O potential.[57]

3. Results and Discussion

3.1. Static Properties. The most important simulation results for the lithium hydration at different concentrations and temperatures are collected in Tables 3 and 4, respectively. The energetics from the simulations is gathered first in these two tables, divided to both total and water−water, Li^+−water, and Li^+-Cl^- contributions, respectively. From Table 3, we can see that the Dang potential gives the lowest hydration energies at the lower end of concentrations, while at the highest concentrations, the exponential EAI potential seems to be energetically most stable. The reason for this is discussed below in connection to the hydration structure. As the temperature is varied for the 1.7 *m* concentrations, all three potentials behave similarly as can be seen from Table 4.

Examples of lithium−water and lithium−chloride radial distribution functions (RDFs), calculated at two concentrations,

TABLE 4: Some Properties of Aqueous LiCl Solution Calculated at Different Temperatures[a]

Li^+-H_2O potential	temperature, K								
	243	263	283	298	303	323	343	363	383
	E_{tot}/N_{tot}, kJ/mol								
D	−73.5	−72.3	−71.1	−70.2	−70.0	−68.8	−68.0	−67.0	−66.1
H	−70.1	−68.9	−67.7	−66.8	−66.6	−65.5	−64.6	−63.6	−62.8
E	−70.8	−69.5	−68.4	−67.6	−67.3	−66.2	−65.3	−64.4	−63.5
	$E(H_2O-H_2O)/N_{H_2O}$, kJ/mol								
D	−42.2	−38.9	−36.4	−34.2	−33.4	−32.9	−30.4	−29.7	−28.6
H	−42.1	−37.9	−35.9	−34.5	−34.0	−32.0	−31.1	−30.0	−29.0
E	−43.2	−39.7	−36.1	−34.7	−34.0	−32.2	−30.8	−29.4	−28.7
	$E(Li-H_2O)/N_{Li}$, kJ/mol								
D	−537	−542	−574	−557	−586	−516	−571	−569	−578
H	−473	−520	−529	−508	−514	−520	−517	−516	−502
E	−464	−506	−541	−533	−523	−529	−532	−524	−604
	$E(Li-Cl)/N_{Li}$, kJ/mol								
D	−985	−977	−929	−972	−937	−1032	−926	−967	−962
H	−944	−914	−885	−900	−891	−891	−895	−913	−900
E	−961	−918	−882	−914	−910	−903	−912	−891	−821
	Coordination Number of Li^+								
D	3.78	3.89	3.97	3.90	4.10	3.75	4.08	4.06	4.18
H	5.26	5.60	5.57	5.40	5.46	5.41	5.38	5.31	5.35
E	3.84	3.83	3.95	3.98	4.01	4.00	4.04	4.06	4.05
	H_2O Self-Diffusion Coefficients (10^{-5} cm^2/s)								
D	0.25	0.64	1.15	1.70	1.84	2.76	3.59	4.73	5.68
H	0.27	0.63	1.17	1.69	1.92	2.71	3.75	4.60	5.67
E	0.29	0.65	1.15	1.73	1.92	2.72	3.65	4.72	5.62
	Li^+ Self-Diffusion Coefficients (10^{-5} cm^2/s)								
D	0.08	0.25	0.39	0.74	0.71	1.33	1.42	1.79	2.29
H	0.10	0.24	0.49	0.68	0.71	1.07	1.40	2.27	2.28
E	0.11	0.30	0.48	0.63	0.78	1.04	1.84	2.22	2.83
	H_2O-Li^+ Residence Times (ps)								
D	90.1	56.6	41.0	30.3	27.5	22.6	17.4	14.1	11.6
H	55.8	36.9	25.2	18.1	17.4	12.9	10.6	8.6	7.2
E	82.8	49.4	33.5	25.5	22.8	16.0	13.2	10.3	8.6

[a] Notation: D = Dang parameters;[30] H = Heinzinger parameters;[48] E = our own exponential ab initio-based Li^+-H_2O potential.[57]

are shown in Figures 1 and 2, respectively. For a comparison, we have also added the total Li^+ radial distribution derived from recent neutron diffraction measurements.[3] We can see from the figures that the simulation results obtained using the Lennard-Jones lithium−water potential with Dang's parameters and using our exponential EAI potential both predict the positions of the maxima of Li^+-H_2O RDF in good agreement with the diffraction experiments, as well as with the data of ab initio MD.[57] For the Heinzinger potential, the maxima are shifted further away by about 0.3−0.4 Å, roughly to a region where the minima are located for the other models, including the experiment. Both the Dang and EAI potential give 4 as the coordination number, while the Heinzinger potential gives 6, which is also reflected in the position of the maxima. To arrange six water molecules around the cation pushes the negatively charged oxygens further away. The question of the correct coordination number is confusing. Our simulations with the EAI and Dang models give the same Li^+-O and Li^+-H distances as the recent experiments by Howell and Neilson using neutron diffraction with isotopic substitution (NDIS).[3] However, they interpret their results to give a coordination number of 6 at the concentrations treated in our simulations. However, it is obvious for us that we cannot have more than four water molecules by retaining the same ion−water distances. On the other hand, the Heinzinger potential in our simulations gives 6 as the coordination number, but we can see from the RDFs that it also requires longer ion−oxygen and ion−hydrogen distances. The older (and less accurate) diffraction experiments by Ichikawa et al.[71] and Narten et al.[72] give coordination number 4. It should be pointed out, however, that

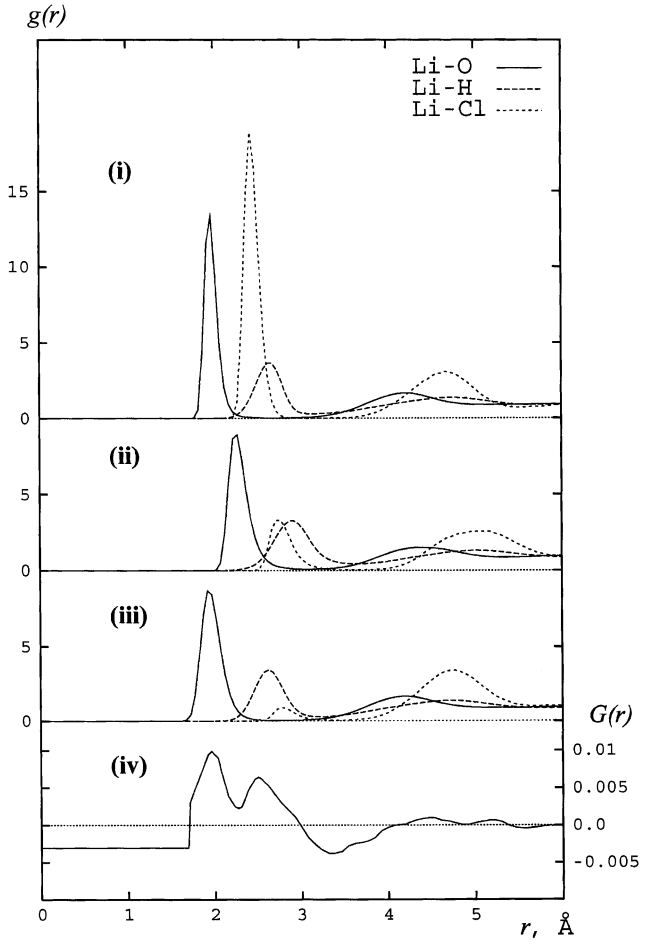

Figure 1. Li^+ radial distribution functions for 1 *m* solution of lithium chloride in water at 25 °C: (i) calculated RDFs obtained using Lennard-Jones potential with parameters of Dang; (ii) calculated RDFs obtained using Lennard-Jones potential with parameters of Heinzinger; (iii) RDF calculated using our own lithium−water exponential EAI potential; (iv) the total Li^+ radial distribution function, $G(r)$, derived from neutron diffraction experiments (reproduced from ref 3).

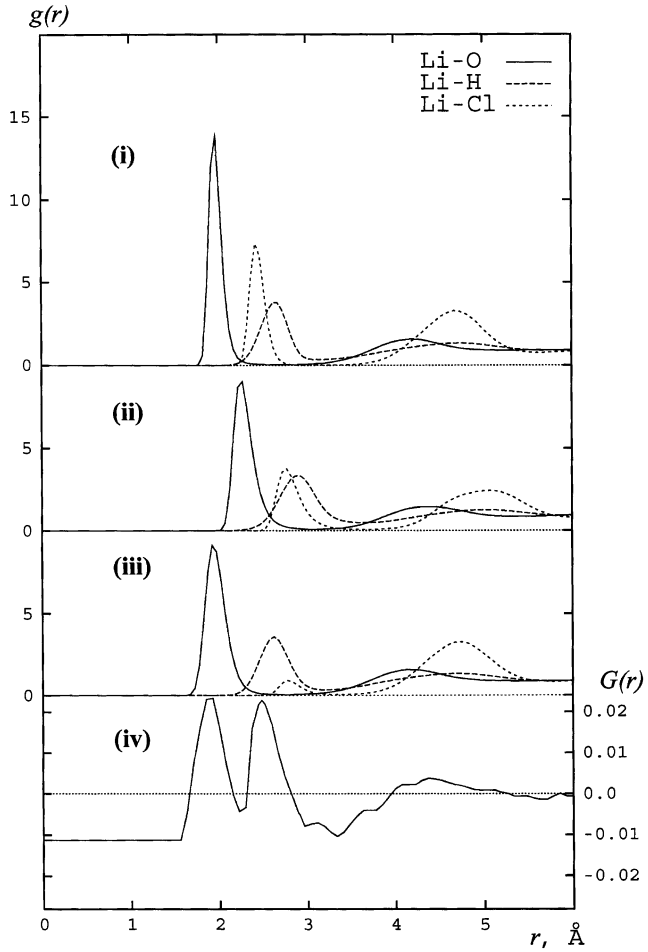

Figure 2. The Li^+ radial distribution functions for a 3.6 *m* solution of lithium chloride in water at 25 °C: (i) calculated RDFs obtained using Lennard-Jones potential with parameters of Dang; (ii) calculated RDFs obtained using Lennard-Jones potential with parameters of Heinzinger; (iii) RDF calculated using our own lithium−water exponential EAI potential; (iv) the total Li^+ radial distribution function, $G(r)$, derived from neutron diffraction experiments (reproduced from ref 3).

in the case of ref 71 the authors unsurprisingly found a value of 2.3 for n_{Li} in a very concentrated solution, while in ref 72 (an X-ray and neutron study at the total diffraction level), the authors had to model their data. Moreover, X-rays are only weakly scattered by Li^+ and correlations between Li^+ and O atoms are not strongly evident in the total scattering patterns of the solution.

While our EAI model[57] and the Dang model[30] both yield rather similar ion−water distribution functions, the ion−ion distributions turned out to be rather different. The first peak of the LiCl RDF becomes much more pronounced in the case of the Dang model (see Figures 1 and 2). The structure of the lithium hydration shell contributes to creation of the ion pairs. The exponential EAI potential is significantly smoother than the Lennard-Jones type of potentials (for illustration, see Figure 9 in ref 57); the electrostatic interactions are softened by the nonelectrostatic part of the potential more efficiently. Because of this effect, the lithium ion hydration shell is inserted much better in the hydrogen-bond network of water.

A much more detailed view on the hydration structure of the Li^+ hydration shell can be given using the density maps of water oxygen distributions shown in Figures 3−5 for the three models—EAI, Dang, and Heinzinger, respectively. The density maps show distribution of a water molecule relative to Li^+ ion together with another water molecule in the first hydration shell. In the case of the exponential EAI potential (Figure 3), the tetrahedral structure, typical for a bulk water, is well-pronounced. This can be interpreted that the lithium ion fits perfectly in the hydrogen-bonded water structure because the Li^+ needs effectively an equal amount of space as do the water molecules. One can clearly see the maxima of water oxygen distribution at the tetrahedral positions around the Li^+−O pair. This result coincides with the data from the ab initio simulations (see Figure 6). The simulation with the Heinzinger potential[48] shows clearly an octahedral hydration structure with maxima corresponding to 90° and 180° O−Li−O angle. An interesting effect is observed for the Dang potential (Figure 4). Namely, while the principal maxima of the density map corresponds to a tetrahedral structure, there is another weaker maximum corresponding to O−Li−O angle of 180°, which is typical for the octahedral structure. So, while the Dang potential gives a coordination number of exactly 4, the structure of the hydration shell is not always strictly tetrahedral but can sometimes adopt even other configurations with two waters along the same line with the Li^+ ions. The exponential EAI potential also provides a hydration number of 4 but keeps strictly the tetragonal structure as it was observed in ab initio simulations.[57]

To investigate the possibility for a 6-fold water coordination around lithium, Car−Parrinello molecular dynamics simulations of 32 water molecules and one Li^+ cation in a periodic box

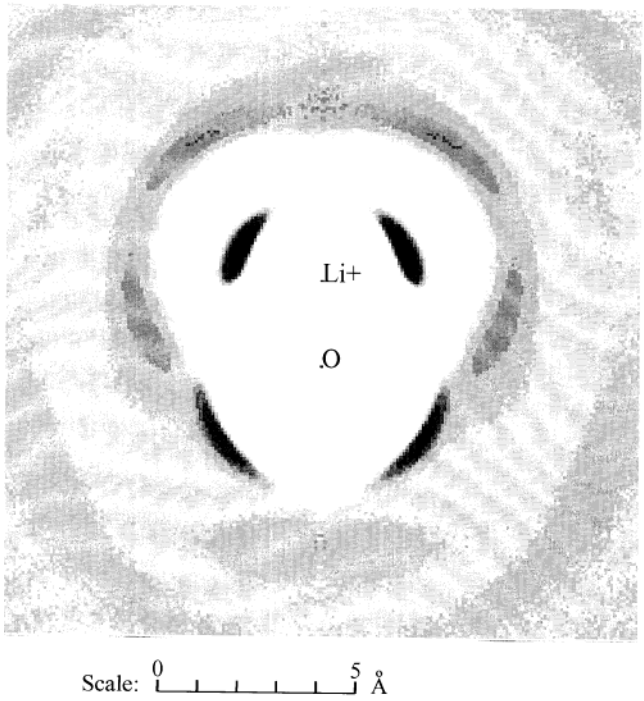

Figure 3. Distribution of water oxygen density around fixed Li^+-O pair in 1.7 *m* LiCl solution calculated at 25 °C using the exponential EAI lithium−water potential.[1] The density of the distribution points is proportional to oxygen density.

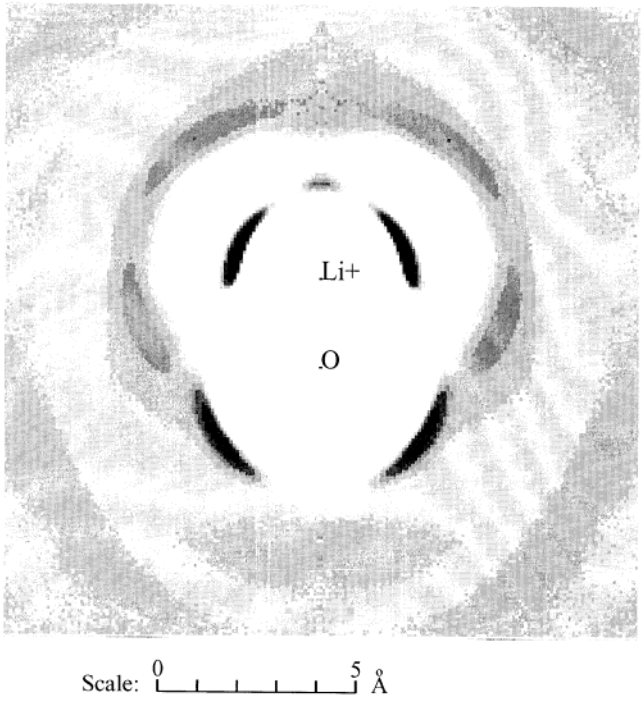

Figure 4. Distribution of water oxygen density around fixed Li^+-O pair in 1.7 *m* LiCl solution calculated at 25 °C using Lennard-Jones type lithium−water potential with Dang's parameters. The density of the distribution points is proportional to oxygen density.

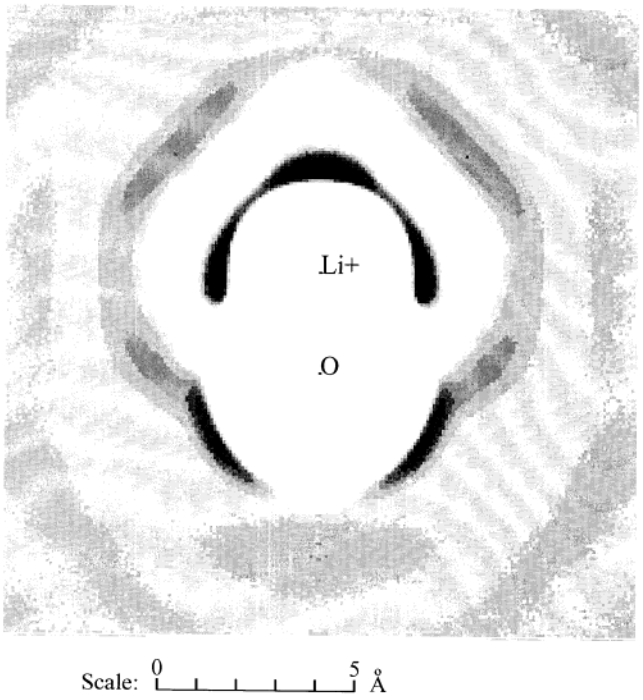

Figure 5. Distribution of water oxygen density around fixed Li^+-O pair in 1.7 *m* LiCl solution calculated at 25 °C using Lennard-Jones type lithium−water potential with Heinzinger's parameters. The density of the distribution points is proportional to oxygen density.

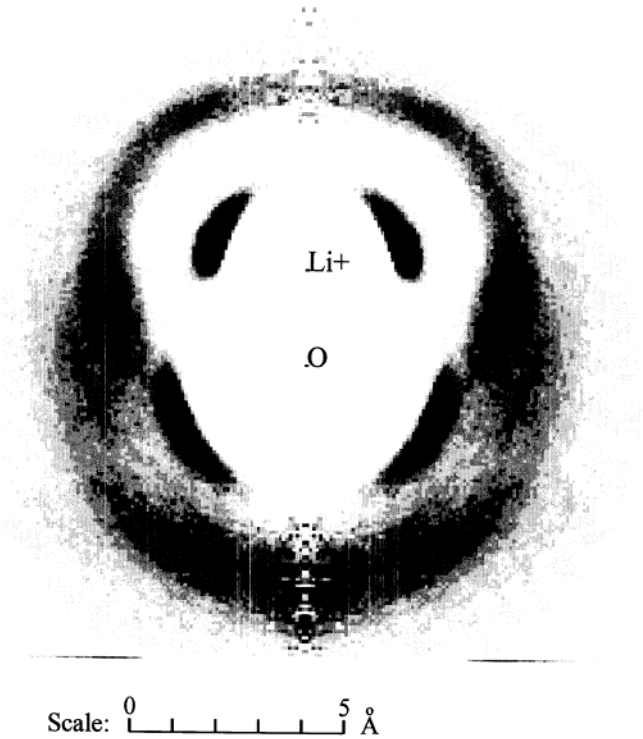

Figure 6. Distribution of water oxygen density around fixed Li^+-O pair obtained from Car−Parinello MD simulations at 25 °C (for other simulation details, see ref 57). The density of the distribution points is proportional to oxygen density.

were carried out (Figure 6). Full description of the simulation details can be found in ref 57. The initial configuration was taken from a classical molecular dynamics simulation of the same system. An ideal octahedron of SPC/E-water molecules was constructed around the cation. Because the quantum-chemical calculations[53,73] give the lithium−oxygen distance within a range of from 1.94 to 2.16 Å for the octahedral structure depending of the level of theory, we chose the distance of 2 Å in our simulations. As a next step, the structure was placed in the center of a periodic box with the additional 26 water molecules. The positions of the oxygens in the octahedron were fixed, and the system was equilibrated during the 200 ps at the temperature of 363 K. This particular temperature was chosen

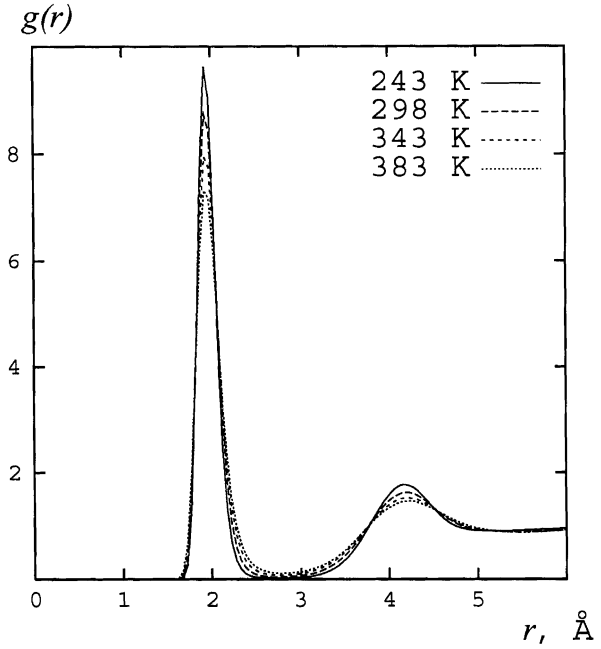

Figure 7. The lithium−water oxygen radial distribution functions for 1.7 *m* aqueous solution of lithium chloride calculated at different temperatures. The simulations were carried out using the exponential EAI lithium−water interaction potential.

because recent NMR relaxation studies in aqueous LiCl solution[5] suggest a 6-fold structure of the first coordination shell around the lithium at temperatures above 40 °C. Also, the higher temperature gives a less-stable four-coordinated hydration shell as can be seen in Table 4, which would in turn promote a possible six-coordination.

However, when the Car−Parrinello MD simulation was started, an immediate destruction of water octahedron was observed. Already after 1.0 ps of simulation, the water structure around the lithium ion became fully tetrahedral. From these ab initio computer simulations, it is not clear how six water molecules can be accommodated around the Li^+ ion while keeping the distance between the ion and water's oxygens equal or below 2 Å.

Another distinct feature of the exponential EAI potential is its weak sensitivity to the salt concentration. The decrease of the lithium coordination number with the salt concentration is significanly less-pronounced for EAI than in potentials of Lennard-Jones type (see Table 3). In the case of both Lennard-Jones potentials, there is a quite significant peak in the LiCl RDF, corresponding to a formation of contact ion pairs. This is increasing with the salt concentration. When Cl^- ions come into a contact with Li^+ ions, replacing water molecules in the hydration shell, it also leads also to a decrease of the hydration number. In the case of the exponential EAI potential, the tetrahedral hydration shell of Li^+ ion remains nearly unperturbed, even at highest ion concentrations.

Temperature variation has only a slight effect on lithium hydration. A typical example of the Li^+−O distribution function at different temperatures is shown in Figure 7. Within the considered temperature range, the RDFs are very similar to each other. The simulations demonstrate that for all three potentials, the coordination number of lithium cation hardly depends on the temperature (see Table 4). These results are in agreement with experimental data from both X-ray and neutron diffraction studies.[74,75] It should be pointed out that the information on hydration numbers contained in these papers corresponds to aqueous solutions with large concentrations of salt. Again,

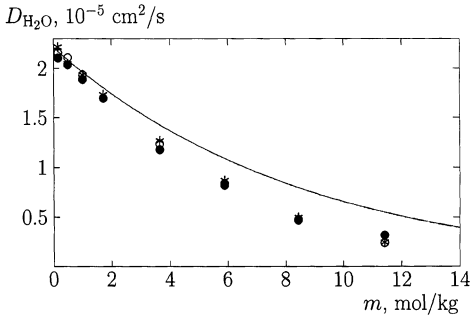

Figure 8. Concentration dependence of water self-diffusion coefficient in LiCl aqueous solution at room temperature. Symbols ○, ●, and ∗ denote the result of simulation using the Dang's, the Heinzinger's, and the exponential lithium−water potentials, respectively; the solid line represents the experimental data from ref 76.

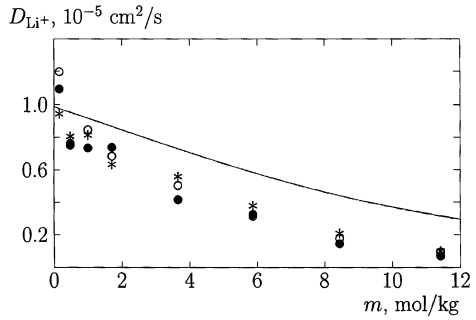

Figure 9. Concentration dependence of lithium ion self-diffusion coefficient in LiCl aqueous solution at room temperature. Symbols ○, ●, and ∗ denote the result of simulation using the Heinzinger's, the Dang's, and the exponential EAI lithium−water potentials, respectively; the solid line represents the experimental data from ref 77.

unsurprisingly one might expect the coordination number of Li^+ to be relatively low for a solution with $D_2O/LiCl = 5$.

3.2. Dynamical Properties. Molecular dynamics simulations allow time-dependent properties of the molecules to be calculated. In this work, we have only considered two dynamical properties: the self-diffusion and residence times of the hydrating water molecules. Both are calculated as a function of concentration and temperature.

The concentration dependence of the calculated and experimental self-diffusion coefficients are shown in Figures 8 and 9 for water and the lithium ion, respectively, at room temperature. We can see from Figure 8, that different ion models have nearly same impact on water diffusion, which is an average of those for bound and bulk water in the simulation cell. The agreement between the simulations and the experiment is better at dilute to low concentrations because the SPC/E model itself gives a good diffusion coefficient for pure liquid water. Overall, the water diffusion is slightly lower in simulations compared to experiment. In the case of Li^+ diffusion, there is a larger mutual scattering of the values at the lowest concentrations, most likely due to a statistical uncertainty. The overall concentration dependence is reproduced although the simulated self-diffusion coefficients are quite significantly smaller than the experimental values.

Temperature dependence is similarly given in Figures 10 and 11 for the 1.7 *m* LiCl solution. Again, one can see that in all cases, the simulation results are more similar to each other than to the experimental data. The diffusion coefficients are systematically lower than experimental values. The data on the temperature dependence of water self-diffusion, shown in Figure 10, demonstrate that the SPC/E water model describes the temperature effects on water diffusion in moderately (1.7 mol/

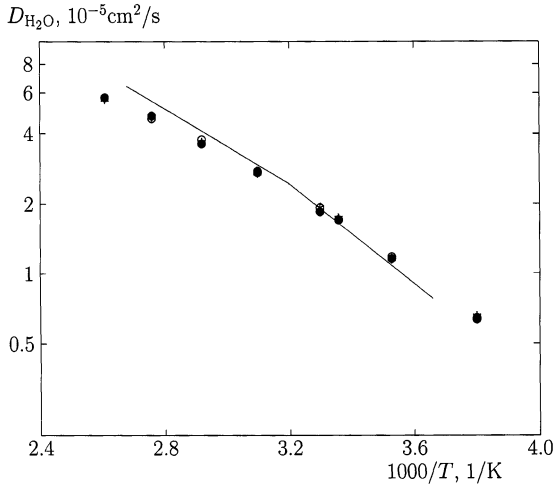

Figure 10. Temperature dependence of water self-diffusion coefficient in 1.7 *m* LiCl aqueous solution. Symbols ○, ●, and ∗denote the result of simulation using the Heinzinger's, the Dang's, and the exponential lithium−water potentials, respectively; the solid line represents the experimental data for 2.0 *m* LiCl solution taken from ref 78.

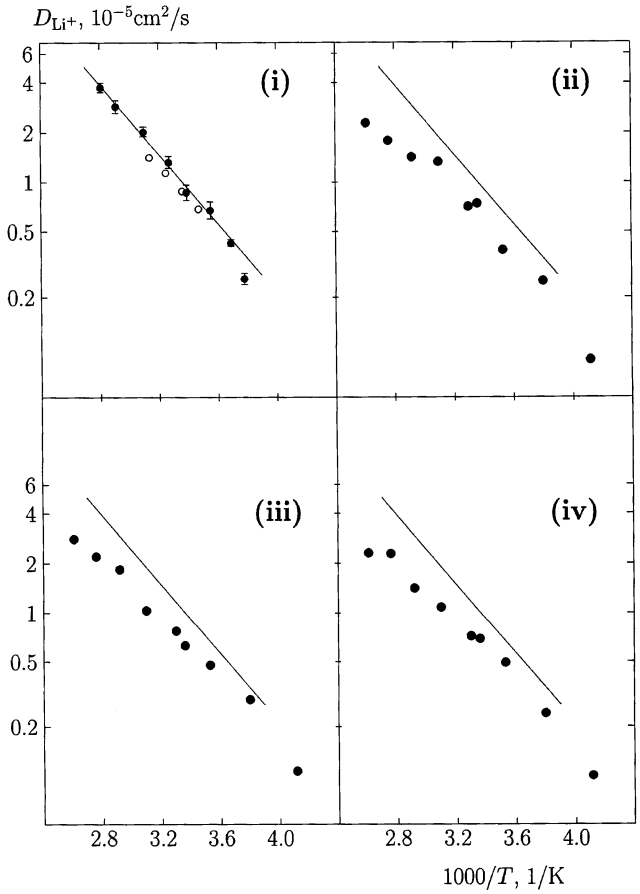

Figure 11. Temperature dependence of a lithium ion self-diffusion coefficient in 1.7 *m* LiCl aqueous solution: (i) our experimental NMR data, fitted to a line, which is also drawn in panels ii, iii, and iv showing the simulation results (see below). The experimental point at the lowest temperature was excluded from the fitting procedure because of the freezing of the sample. The ○ symbols in panel i denote the experimental data for 2.0 *m* LiCl solution obtained using the diaphragm cell method.[79] Panel iii shows the results from the simulations using lithium−water exponential EAI potential; Panels ii and iv show the results using Lennard-Jones potential with parameters of Dang and Heinzinger, respectively.

kg) concentrated solutions well. On the other hand, the calculated self-diffusion coefficients of lithium ion (see Figure 11) are systematically lower than the experimental ones. Moreover, the slopes of the simulated temperature dependences differ somewhat from the experimental slope. Because the temperature dependence of water diffusion is well reproduced in the simulations but not the ion diffusion, it means that none of the models do particularly good work to provide reliable diffusion coefficients over the considered temperature interval.

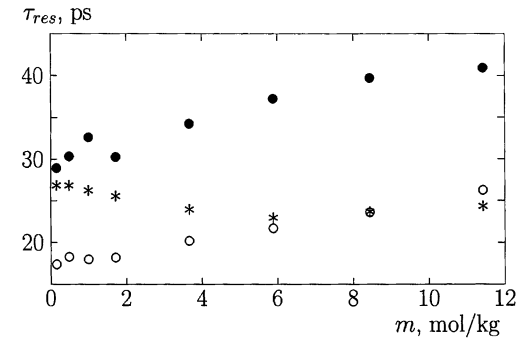

Figure 12. Concentration dependence of the residence time of water molecules in the lithium hydration shell in LiCl aqueous solution at room temperature. Symbols ○, ●, and ∗denote the results of simulation using the Heinzinger's, the Dang's, and the exponential lithium−water potentials, respectively.

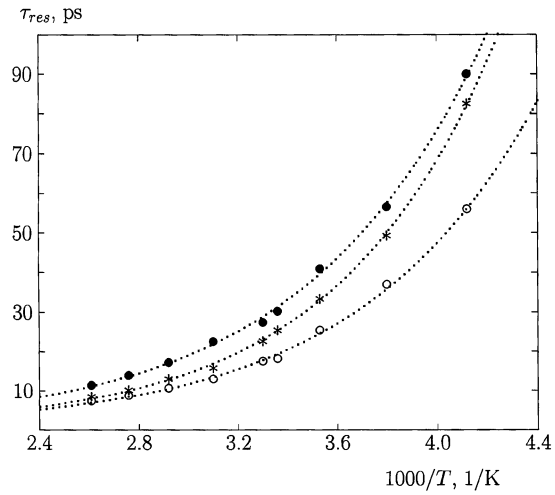

Figure 13. Temperature dependence of the residence time of water molecules in the lithium hydration shell in 1.7 *m* LiCl aqueous solution. Symbols ○, ●, and ∗denote the results of simulation using the Heinzinger's, the Dang's, and the exponential lithium−water potentials, respectively. The dotted lines are the approximation of the simulation results by the $A \exp(E/(kT))$ function.

For the residence times of water molecules in the Li^+ hydration shell, one can see the different sensitivity of the potentials used to the salt concentration: the residence time is increasing with the salt concentration for Dang and Heinzinger potentials, while it remains practically constant (or even slightly decreasing) for the exponential EAI potential (see Table 3 and Figure 12).

The effect of temperature on the residence time of water molecules in the lithium hydration shell is described well by a simple exponential, $A \exp(E/(kT))$, function, where E is the energy required for an exchange of water between the ion hydration shell and bulk water. The simulation results together with approximation curves are shown in Figure 13. We estimated the parameter E as 12.9 ± 0.2 kJ/mol for exponential Li^+−water potential and as 11.5 ± 0.2 and 11.7 ± 0.2 kJ/mol for Lennard-Jones potential with Dang's and Heinzinger's parameters, correspondingly.

4. Conclusions

In the present work, several key details of microstructure and kinetic properties of lithium cation hydration shell have been studied by classical MD simulations and to a smaller extent complemented with Car−Parrinello simulations. The aqueous LiCl solution has been simulated in a wide range of concentrations (from 0.1 to 11.4 mol/kg) and temperatures (from −30 to 110 °C) for three interaction potentials. Although this investigation is far from being complete, the obtained, systematically simulated results allow us to point out a few important observations.

The microstructure of the lithium hydration shell depends very strongly on the lithium−water interaction parameters. Simulations with our own exponential EAI potential provide a hydration structure that is very similar to that obtained in the ab initio simulations. Of course, it should do so because the potential was created from the RDFs obtained in the ab initio simulations using the method of inverse Monte Carlo.[58] The exponential EAI potential gives a much more pronounced tetrahedral hydration structure of the Li^+ ion, observed also in the Car−Parrinello simulations, and it is kept even at high salt concentrations. These results concerning the hydration structure, obtained in this work, encourage the use of the method of inverse Monte Carlo to construct effective interaction potentials from ab initio simulations, as was suggested in refs 57 and 59.

For the self-diffusion of Li^+, the results seem less conclusive. Neither the standard potentials of Lennard-Jones type nor the exponential EAI potential derived from ab initio calculations was able to quantitatively reproduce both the concentration and temperature effects on lithium ion diffusion, leading to a slower Li^+ diffusion at high salt concentrations. One can see that the ab initio-based potential now works equally well as the empirical potentials of Lennard-Jones type. The approach to construct simple effective pair potentials using data from limited size but accurate first principles simulations and use the potentials in classical full scale simulations, beyond the capabilities of CPMD or other ab initio simulation schemes, has a great potential to become a general and simple recipe. The basic idea in the inverse Monte Carlo scheme[58] can be used to construct both nonbonded and bonded interaction potentials, as well as solvent-mediated interaction potentials with the microscopic solvation structure implicitely included.

During the review of our paper, two excellent papers dealing with hydration of Li^+ have appeared[80,81] and should be cited here. Results from these papers do not alter our conclusions.

Acknowledgment. This work has been supported by Russian Foundation for Basic Research (Grant 01-03-32768), by The Grant Center for the Natural Sciences (Grant PD02-1.2.-3), and by The Swedish Science Research Council (VR).

References and Notes

(1) Friedman, H. L. *Chem. Scr.* **1985**, *25*, 42.
(2) Ohtaki, H.; Radnai, T. *Chem. Rev.* **1993**, *93*, 1157.
(3) Howell, I.; Neilson, G. W. *J. Phys.: Condens. Matter* **1996**, *8*, 4455.
(4) Rudolph, W.; Brooker, M. H.; Pye, C. C. *J. Phys. Chem.* **1995**, *99*, 3793.
(5) Chizhik, V. I. *Mol. Phys.* **1997**, *90*, 653.
(6) Heinzinger, K.; Vogel, P. C. *Z. Naturforsch. A* **1974**, *29*, 1164.
(7) Heinzinger, K.; Vogel, P. C. *Z. Naturforsch. A* **1976**, *31*, 463.
(8) Clementi, E.; Barsotti, R.; Fromm, J.; Watts, R. O. *Theor. Chim. Acta* **1976**, *43*, 101.
(9) Clementi, E.; Barsotti, R. *Chem. Phys. Lett.* **1978**, *59*, 21.
(10) Szasz, G. I.; Heinzinger, K.; Riede, W. O. *Z. Naturforsch. A* **1981**, *36*, 1067.
(11) Szasz, G. I.; Heinzinger, K.; Riede, W. O. *Ber. Bunsen-Ges. Phys. Chem.* **1981**, *85*, 1056.
(12) Engström, S.; Jönsson, B. *Mol. Phys.* **1981**, *43*, 1235.
(13) Mezei, M.; Beveridge, D. L. *J. Chem. Phys.* **1981**, *74*, 6902.
(14) Engström, S.; Jönsson, B.; Jönsson, B. *J. Magn. Res.* **1982**, *50*, 1.
(15) Impey, R. W.; Madden, P. A.; McDonald, I. R. *J. Phys. Chem.* **1983**, *87*, 5071.
(16) Okada, I.; Kitsuno, Y.; Lee, H.-G.; Ohtaki, H. *Stud. Phys. Theor. Chem.* **1983**, *27*, 81.
(17) Szasz, G. I.; Heinzinger, K. *J. Chem. Phys.* **1983**, *79*, 3467.
(18) Bopp, P.; Okada, I.; Ohtaki, H.; Heinzinger, K. *Z. Naturforsch. A* **1984**, *40*, 116.
(19) Chandrasekhar, J.; Spellmeyer, D. C.; Jorgensen, W. L. *J. Am. Chem. Soc.* **1984**, *106*, 903.
(20) Nguyen, H. L.; Adelman, S. A. *J. Chem. Phys.* **1984**, *81*, 4564.
(21) Bounds, D. G. *Mol. Phys.* **1985**, *54*, 1335.
(22) Pettitt, B. M.; Rossky, P. J. *J. Chem. Phys.* **1986**, *84*, 5836.
(23) Mills, M. F.; Reimers, J. R.; Watts, R. O. *Mol. Phys.* **1986**, *57*, 777.
(24) Tanaka, K.; Ogita, N.; Tamura, Y.; Okada, I.; Ohtaki, H.; Palinkas, G.; Spohr, E.; Heinzinger, K. *Z. Naturforsch. A* **1987**, *42*, 29.
(25) Tamura, Y.; Tanaka, K.; Spohr, E.; Heinzinger, K. *Z. Naturforsch. A* **1988**, *43*, 1103.
(26) Reddy, M. R.; Berkowitz, M. *J. Chem. Phys.* **1988**, *88*, 7104.
(27) Cieplak, P.; Kollman, P. *J. Chem. Phys.* **1990**, *92*, 6761.
(28) Auffinger, P.; Wipff, G. *J. Am. Chem. Soc.* **1991**, *113*, 5976.
(29) Romero, C. *J. Chim. Phys.* **1991**, *88*, 765.
(30) Dang, L. X. *J. Chem. Phys.* **1992**, *96*, 6970.
(31) Lee, S. H.; Rasaiah, J. C. *J. Chem. Phys.* **1994**, *101*, 6964.
(32) Llano-Restrepo, M.; Chapman, W. G. *J. Chem. Phys.* **1994**, *100*, 8322.
(33) Odelius, M.; Kowalewski, J. *J. Chem. Soc., Faraday Trans. 1* **1995**, *91*, 215.
(34) Lee, S. H.; Rasaiah, J. C. *J. Phys. Chem.* **1996**, *100*, 1420.
(35) Obst, S.; Bradaczek, H. *J. Phys. Chem.* **1996**, *100*, 15677.
(36) Toth, G. *J. Chem. Phys.* **1996**, *105*, 5518.
(37) Degreve, L.; de Pauli, M. V.; Duarte, M. A. *J. Chem. Phys.* **1997**, *106*, 655.
(38) Flanagin, L. W.; Balbuena, P. B.; Johnston, K. P.; Rossky, P. J. *J. Phys. Chem. B* **1997**, *101*, 7998.
(39) Periole, X.; Allouche, D.; Daudey, J.-P.; Sanejouand, Y.-H. *J. Phys. Chem. B* **1997**, *101*, 5018.
(40) Periole, X.; Allouche, D.; Ramirez-Solis, A.; Ortega-Blake, I.; Daudey, J. P.; Sanejouand, Y. H. *J. Phys. Chem. B* **1998**, *102*, 8579.
(41) Tongraar, A.; Liedl, K. R.; Rode, B. M. *Chem. Phys. Lett.* **1998**, *286*, 56.
(42) Koneshan, S.; Rasaiah, J. C.; Lynden-Bell, R. M.; Lee, S. H. *J. Phys. Chem. B* **1998**, *102*, 4193.
(43) Hermansson, K.; Wojcik, M. *J. Phys. Chem. B* **1998**, *102*, 6089.
(44) Babu, C. S.; Lim, C. *J. Phys. Chem. B* **1999**, *103*, 7958.
(45) Egorov, A. V.; Komolkin, A. V.; Chizhik, V. I. *J. Mol. Liq.* **2001**, *89*, 47.
(46) Fisher, W.; Brickmann, J. *Ber. Bunsen-Ges. Phys. Chem.* **1982**, *86*, 650.
(47) Kollman, P. A.; Wipff, G.; Chandra Singh, U. *J. Am. Chem. Soc.* **1985**, *107*, 2212.
(48) Heinzinger, K. *Physica B* **1985**, *131*, 196.
(49) Sung, S.-S.; Jordan, P. C. *J. Chem. Phys.* **1986**, *85*, 4045.
(50) Åqvist, J. *J. Phys. Chem.* **1990**, *94*, 8021.
(51) Kistenmacher, H.; Popkie, H.; Clementi, E. *J. Chem. Phys.* **1973**, *59*, 5842.
(52) Pye, C. C.; Rudolph, W.; Poirier, R. A. *J. Phys. Chem.* **1996**, *100*, 601.
(53) Pye, C. C. *Int. J. Quantum Chem.* **2000**, *76*, 62.
(54) Rempe, S. B.; Pratt, L. R.; Hummer, G.; Kress, J. D.; Martin, R. L.; Redondo, A. *J. Am. Chem. Soc.* **2000**, *122*, 966.
(55) Bischof, G.; Silbernagl, A.; Hermansson, K.; Probst, M. *Int. J. Quantum Chem.* **1997**, *65*, 803.
(56) Izvekov, S.; Philpott, M. R. *J. Chem. Phys.* **2000**, *113*, 10676.
(57) Lyubartsev, A. P.; Laasonen, K.; Laaksonen, A. *J. Chem. Phys.* **2001**, *114*, 3120.
(58) Lyubartsev, A. P.; Laaksonen, A. *Phys. Rev. E* **1995**, *52*, 3730.
(59) Lyubartsev, A. P.; Laaksonen, A. *Chem. Phys. Lett.* **2000**, *325*, 15.
(60) Nosé, S. *Mol. Phys.* **1984**, *52*, 255.
(61) Martyna, G. J.; Tobias, D. J.; Klein, M. L. *J. Chem. Phys.* **1994** *101*, 4177.
(62) *CRC Handbook of Chemistry and Physics*; Weast, R. C., Lide, D. R., Eds.; CRC Press: Boca Raton, FL, 1989.
(63) Berendsen, H. J. C.; Grigera, J. R.; Straatsma, T. P. *J. Phys. Chem.* **1987**, *91*, 6269.

(64) Baez, L. A.; Clancy, P. *J. Chem. Phys.* **1994**, *101*, 9837.
(65) Starr, F. W.; Sciortino, F.; Stanley, H. E. *Phys. Rev. E* **1999**, *60*, 6757.
(66) Smith, D. E.; Dang, L. X. *J. Chem. Phys.* **1994**, *100*, 3757.
(67) Lyubartsev, A. P.; Laaksonen, A. *J. Phys. Chem.* **1996**, *100*, 16410.
(68) Mills, R.; Lobo, V. M. M. *Self-Diffusion in electrolyte solutions*; Physical Sciences Data 36; Elsevier: Amsterdam, The Netherlands, 1989.
(69) Stilbs, P. *Prog. Nucl. Magn. Reson. Spectrosc.* **1987**, *19*, 1.
(70) Mills, R. *J. Phys. Chem.* **1973**, *77*, 685.
(71) Ichikawa, K.; Kaneda, Y.; Matsumoto, T.; Misawa, M. *J. Phys. C: Solid State Phys.* **1984**, *17*, L725.
(72) Narten, A. H.; Vaslow, F.; Levy, H. A. *J. Chem. Phys.* **1973**, *58*, 5017.
(73) Hashimoto, K.; Kamimoto, T. *J. Am. Chem. Soc.* **1998**, *120*, 3560.
(74) Yamagami, M.; Yamaguchi, T.; Wakita, H.; Misava, M. *J. Chem. Phys.* **1994**, *100*, 3122.
(75) Yamanaka, K.; Yamagami, M.; Takamuku, T.; Yamaguchi, T.; Wakita, H. *J. Phys. Chem.* **1993**, *97*, 10835.
(76) Tanaka, K.; Nomura, M. *J. Chem. Soc., Faraday Trans. 1* **1987**, *83*, 1779.
(77) Braun, B. M.; Weingärtner, H. *J. Phys. Chem.* **1988**, *92*, 1342.
(78) Weiss, A.; Nothnagel, K. H. *Ber. Bunsen-Ges. Phys. Chem.* **1971**, *75*, 216.
(79) Andreev, G. A. *Russ. J. Phys. Chem.* **1962**, *36*, 835.
(80) Wahab, A.; Mahuiddin, S. *Can. J. Chem.* **2002**, *80*, 175.
(81) Loeffler, H. H.; Rode, B. M. *J. Chem. Phys.* **2002**, *117*, 110.